Polymers & biopolymers

The effect of high-intensity gamma radiation on PETG and ASA polymer-based fused deposition modelled 3D printed parts

Sam Cressall[1], Chris O. Phillips[1,*] , Wafaa Al-Shatty[2], and Davide Deganello[1]

[1] *Welsh Centre for Printing and Coating, Faculty of Science and Engineering, Swansea University Bay Campus, Fabian Way, Crymlyn Burrows, Swansea SA1 8EN, UK*
[2] *Faculty of Science and Engineering, Swansea University Bay Campus, Fabian Way, Crymlyn Burrows, Swansea SA1 8EN, UK*

ABSTRACT

There is growing interest in the application of 3D printing for demanding environments subject to gamma radiation in areas such as the nuclear industry and space exploration. In this work, the effect of gamma radiation on fused deposition modelled 3D printed parts composed of polyethylene terephthalate glycol (PETG) and acrylic styrene acrylonitrile (ASA) polymers was studied. Dose levels of up to 2.25 MGy were applied to the printed components, doses equivalent to over 1 year operating near spent nuclear fuel cells. Infrared spectroscopy showed the evidence of cross-linking by the formation of peaks corresponding to –OH and C–H bonds. Tensile and hardness testing was used to assess changes in mechanical properties and showed a reduction in ultimate tensile stress and maximum strain in parts made from both polymers, but with PETG retaining greater strength and ductility than ASA, especially at intermediate gamma exposure. Young's modulus and hardness showed either modest increases or a fairly flat response with exposure. Mechanical properties were heavily dependent on the build structure, with horizontal build samples pulled parallel to the filament direction being several times stronger than vertical build samples pulled normal to the layers. Non-irradiated samples pulled parallel to the filament direction were indicative of ductile failure, with rough surfaces, distinct infill and wall regions and evidence of thinning occurring after fracture, but irradiated fracture surfaces were flatter, smoother and without local thinning, suggesting gamma radiation-induced embrittlement in the material. For samples pulled perpendicular to the filament direction, all fractures occurred between layers, creating flat fracture surfaces with no evidence of necking and indicative of brittle failure regardless of whether the samples were irradiated.

Introduction

There is growing interest in the application of fused deposition modelled (FDM) parts in environments subject to gamma radiation. A few examples of these applications include the sterilisation of surgical equipment [1–4], deployment of robotics in the nuclear industry [5, 6] and flexible manufacturing during space missions [7, 8]. As interest in additive manufacturing (AM) in these sectors continues to grow, it will become important to understand the chemical and mechanical response of 3D printed parts exposed to intense gamma radiation.

The chemical mechanisms that occur when gamma-ray radiation is applied to polymers manufactured using traditional methods have been well documented [9]. However, few papers have investigated plyometric AM parts subject to intense gamma radiation, which may react differently to traditionally manufactured polymer response. Regarding irradiation of additively manufactured polymetric parts, the AM process introduces control over part porosity, a control aspect that may well influence the response to radiation.

The primary mechanisms that occur in polymers exposed to radiation are cross-linking and chain scission [10]. Cross-linking increases the complexity of the three-dimensional polymer network, ultimately increasing molecular mass with exposure to radiation [11]. This occurs through the free radicalisation of electrons, which induces oxidation and can eventually lead to the material's embrittlement and degradation [12]. In contrast, chain scission occurs through the breaking of long polymer chains, leading to the material's softening and loss of elastic properties [13]. Many factors can affect the response of a material to radiation, including molecular structure, temperature, dose rate and dissolved oxygen [10]. While exposure to sufficient radiation can substantially weaken materials, in the context of 3D printing, radiation has been used to reduce the inherent anisotropy of 3D printed parts by inducing cross-linking within the microstructure [14].

The magnitude of radiation exposure varies between applications. A typical unit of measurement for radiation exposure is the gray (or Gy), where one gray is a unit radiation dose equivalent to a joule of energy absorbed per kilogram (or 100 rad) [15]. Depending on the application and duration of deployment, the range of dosages experienced by a workforce and/or apparatus will vary substantially. Example dosages for specific applications are listed in Table 1. These vary from an upper extreme in applications such as nuclear incident clean-up using remotely operated vehicles (ROVs) or operating in the vicinity of spent nuclear fuels, which will, at around 5500 Gy/day, amount to over 2 MGy after a year of operation. Sterilisation of polymeric medical devices are typically sterilised to 25 kGy. However, the cumulative nature of radiation can lead to a rise in total exposure over an extended lifetime with multiple sterilisations. Finally, the lowest cited doses are from ambient exposure during space travel.

The rate of oxygen diffusion in a 3D printed part is primarily determined by the porosity, which can be modified at the design stage via printing parameters, specifically infill percentage and orientation [23, 24]. By controlling the rate of oxygen diffusion within the microstructure, tailoring of the radiation-induced chemical process may be possible, with oxygen abundance promoting these chemical changes. Due to the fabrication process, radiation-induced changes in chemistry within 3D printed parts will differ from those experienced by parts manufactured with more traditional methods. Research into the mechanical and chemical changes that occur within 3D printed parts following exposure to gamma radiation has been steadily increasing since 2016; however, the range of materials investigated has been limited. Previous

Table 1 Cited radiation doses for a range of applications

Industry	Application	Dose (Gy/day)	References
Space exploration	Round trip to mars	0.002	[16]
	Previous space missions	220–1270 μ	[17, 18]
Sterilisation of polymeric materials	Poly(vinyl chloride)—food packaging	25000/sterilisation	[3, 19]
	Poly(methyl methacrylate)—medical supplies		
	Polycarbonate—engineering resin		
Nuclear	ROV clean-up and maintenance Fukushima	24000	[6, 20]
	Operating near spent fuel cells	5500	[21, 22]

research has focused on polylactic acid (PLA) [15, 23, 25] and acrylonitrile butadiene styrene (ABS) [23, 26, 27], and historically, these have been the most commonly printed and commercially available materials. However, PLA has been shown to be highly sensitive to even small radiation dosages, making it unsuitable for many long-life operations exposed to radiation. Additionally, ABS has been losing popularity to alternative polymers, due to comparative difficulties in printing compared to the more contemporary materials, with requirements such as actively heated chambers, to reduce warping and cracking, and fume cupboards to remove harmful fumes. Examples of data published on the response of the mechanical properties to gamma radiation (ultimate tensile strength (UTS), maximum strain, Young's modulus and hardness) of PLA and ABS are summarised in Table 2. PLA showed significant degradation in both UTS and maximum strain at exposure levels above 0.05 MGy, while increases in Young's modulus and hardness were recorded up to an exposure of 0.2 MGy. Additionally, papers that reported infrared spectroscopy recorded the formation of a new peak in the 3200–3550 wave number range, corresponding to O–H stretch, with this formation attributed to cross-linking. The discrepancies in Young's modulus between [15] and [23] at exposures above 0.2 MGy could be attributed to the difference in dose rates applied to the materials. In contrast to PLA, ABS has demonstrated a much higher mechanical robustness to gamma radiation. At an equivalent dose of 0.015 MGy, ABS increased in UTS and maximum strain. However, at higher exposures

over 1 MGy, large decreases in the observed UTS and significant decreases in the maximum strain were observed. Increases in hardness and Young's modulus were recorded at all exposure levels.

Polymers containing phenyl groups in the main chain, such as PETG, are known to be more robust to radiation, as the phenyl group absorbs energy, mitigating bond ruptures [12, 13, 28]. Similarly, polymers that contain a benzene ring, such as ASA, are more resistant to radiation than polymers that contain saturated bonds [3, 10, 28, 29]. ASA is well known in the 3D printing community for its excellent weathering resistance, surpassing PLA, ABS and PETG in UV, water and thermal resistivity. ASA is also easier to print than ABS, with less warping and cracking occurring when printing at a larger scale. However, ASA does still require a fume cupboard during printing, as toxic fumes are released due to the generation of styrene.

There is no current research detailing the response of these materials to radiation when used in a 3D printed part. This work therefore investigates the effect of gamma radiation on the mechanical properties of 3D printed parts made from polyethylene terephthalate glycol (PETG) and acrylic styrene acrylonitrile (ASA). Infrared spectroscopy was used to assess chemical changes resulting from radiation exposure. Since 3D printed parts are deposited in layers and exhibit different physical properties depending on whether tension is applied parallel to or normal to the deposited layers, samples were fabricated in both horizontal and vertical builds to focus primarily on

Table 2 Changes in mechanical properties of PLA and ABS as a result of gamma radiation exposure

Material	Dose (MGy)	Percentage of the mechanical property remaining after irradiation compared to control samples				References
		UTS	Max. strain	Young's modulus	Hardness	
PLA	0.03	69.5	62.7	129.5	N/A	[25]
	0.05	83.8	44.0	103.5	101.3	
	0.15	16.8	8.5	110.7	103.9	[15]
	0.2	7.2	3.7	114.3	105.2	
	0.3	7.6	N/A	78.2	N/A	[23]
ABS	0.01	102.9	109.7	107	101.4	[26]
	0.015	103.5	106.9	109	105	[27]
	1	28.8	9.8	122.9	110.3	[26]
	1.4	21.6	4.8	126.8	112.2	
	2.6	37.5	N/A	101.6	N/A	[23]

material tensile strength and fused layer adhesion strength, respectively.

Methodology

Materials

The materials selected for investigation were commercial polyethylene terephthalate glycol (PETG) and acrylic styrene acrylonitrile (ASA) filament from Prusa Research a.s (Czech Republic) as shown in Table 3, with as-printed mechanical properties provided by the supplier. PETG and ASA, whose molecular structures are shown in Fig. 1, are examples of polymers that are growing in use in the sector following relatively recent adoption, with PETG and ASA accounting for 6 and 2% of material use, respectively [30].

3D printing methodology

Samples were printed in batches of 15 using a Prusa I3Mk3 FDM printer (Prusa research a.s.). Samples were designed in SolidWorks and sliced in Ultimaker Cura 4.7 (Ultimaker B.V.). Figure 2 shows the two orientations, relative to the build plate, which were

printed to investigate the response of tensile properties (horizontal build) and layer adhesion strength (vertical build) to gamma radiation. Printing parameters were optimised from practice runs and kept identical between materials, except for the nozzle and build plate temperature, where supplier recommendations were used. Settings are summarised in Table 4.

The polymers were printed to give a dog bone shape suited for tensile testing. The testing cell size constrained the dimensions of the samples within the chamber used to apply the gamma radiation. ISO 527 [31] was used to inform the dimensions of the samples, but the size of each testing cell was $25 \times 25 \times 120$ mm, and five samples were required to fit within each cell (to give sufficient repeat samples for mechanical testing); this limited the length of the samples when compared to the standard. The dimensions of the design, print orientations and resulting printed samples are shown in Fig. 2, with sample length 100 mm, centre section length, width and thickness 32 mm, 6 mm and 4 mm, respectively. The measured dimensions of the printed samples were larger than those designated in the CAD model, which can be attributed to overflow resulting from the 100% infill. The average cross-sectional area of the midsection of the dog bone was 27.3 mm^2 (6.45×4.233 mm). This measurement was

Table 3 Summary of material properties for PLA, PETG and ASA from supplier database

Property	PETG [35]		ASA [36]	
Supplier	Prusa research a.s		Prusa research a.s	
SKU	PRM-PETG-JET-1000		PRM-ASA-JET-850	
Orientation	Horizontal	Vertical	Horizontal	Vertical
UTS (MPa)	47 ± 2	30 ± 5	42 ± 1	9 ± 1
Young's modulus (GPa)	1.5 ± 0.1	1.4 ± 0.1	1.6 ± 0.1	1.4 ± 0.1
Hardness (HV)	15.15 ± 0.75		N/A	
Elongation at break (%)	5.1 ± 0.1	2.5 ± 0.5	3.3 ± 0.1	0.6 ± 0.1
Filament diameter (mm)	1.75 ± 0.02		1.75 ± 0.03	
Cost (£/kg) at time of writing	26.99		31.75	

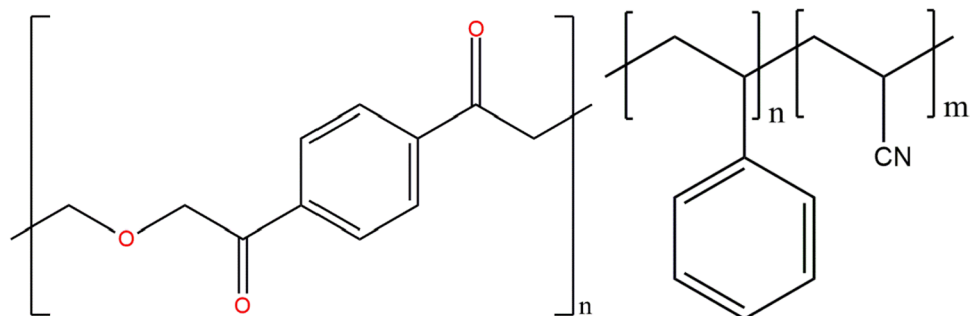**Figure 1** Molecular structure of PETG (LEFT) and ASA (right).

Figure 2 Design dimensions (top) with dimensions in mm, print orientations (middle) and photograph of samples after fabrication (bottom—with vertical sample (top), horizontal sample (bottom)).
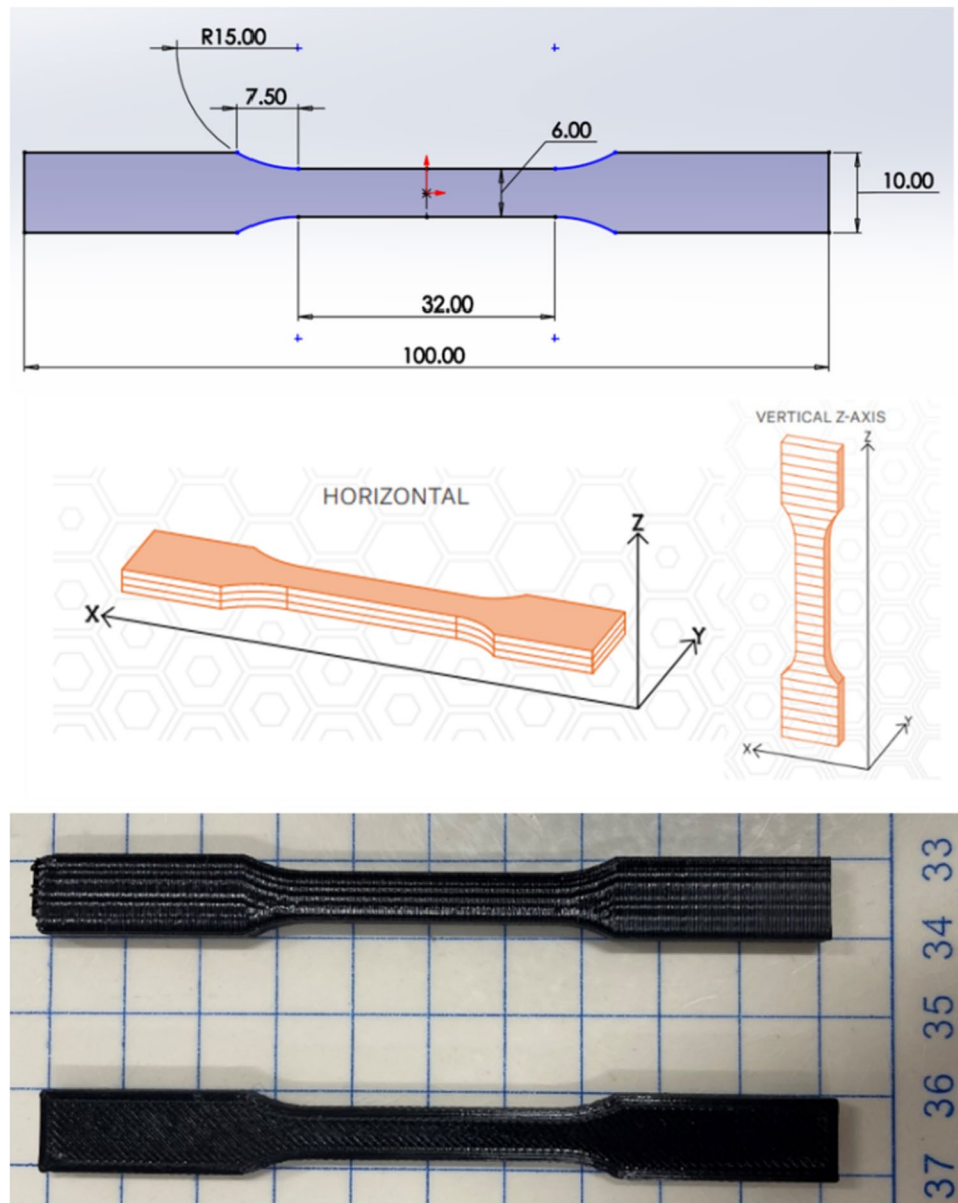

used for mechanical strength calculations. From the Cura slicing profile (Fig. 3), infill and the alternating raster angle of 45° with sequential layers are shown in yellow, the outer wall material is shown in red, and the inner wall material is shown in green. The wall profile was the initial path taken for each layer and followed the perimeter of the layer cross section.

Table 4 3D Printing parameters used in the study

Printing parameter	PETG	ASA
Infill (%)	100	100
Nozzle temp (°C)	260	255
Bed temp (°C)	90	100
Layer height (mm)	0.2	0.2
Raster orientation (°)	±45	±45
Walls	2	2
Print speed (mm/s)	60	60

Irradiation of 3D printed parts

Irradiation of the samples was conducted at the Dalton Cumbrian Facility (DCF) at the University of Manchester. Printed samples were exposed to gamma radiation

Figure 3 Sample orientation slicing profile from Cura. Images **c** i to iv show the change in raster angle with alternating layers.
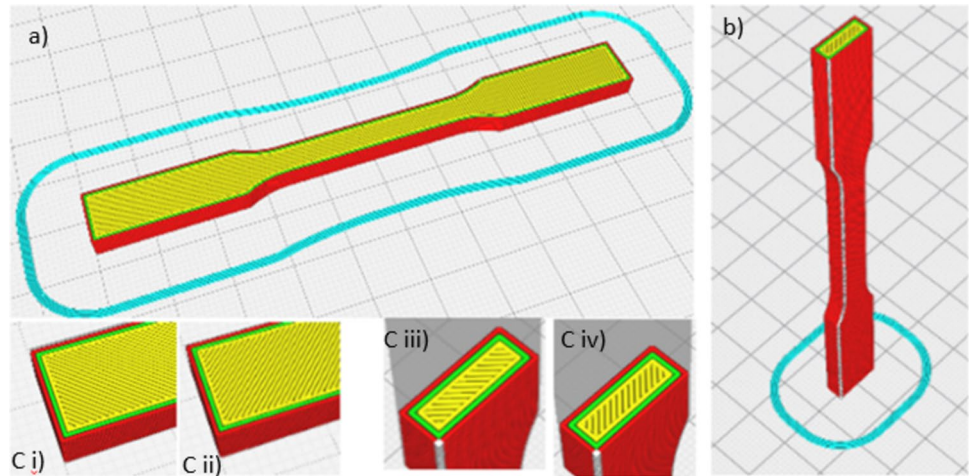
using three high-activity sealed cobalt-60 sources in a Foss Therapy Services Inc. (California, USA) model 812 irradiator at room temperature. Absorbed dose rates in air in the irradiator were determined separately using an ion chamber, calibrated annually to traceable international standards (Radcal Corporation Accu-Dose + base unit equipped with 10X6-0.18 ion chamber with C552 air equivalent walls and electrode). This work employed high radiation exposure levels to mimic extended deployment in highly radioactive zones or multiple sterilisations of medical apparatus. To allow for comparison between materials, PETG and ASA were irradiated to the same exposure, with similar dose rates as listed in Table 5. Samples were irradiated at varying dose rates from 35 to 110 Gy/min. To control the radiation dose, samples were grouped into sets of five and placed in specific cells within the chamber. The distance from the radiation source determined the dose rate. Exposure took around two weeks.

Infrared spectroscopy and mechanical testing of 3D printed parts

Infrared spectroscopy was conducted using a PerkinElmer Frontier FT-IR spectrometer (PerkinElmer,

US) using ATR (attenuated total reflection) configuration. A load of 70N was applied to the samples to ensure consistent contact with the infrared crystal. Five 3D printed parts were tested for each material/exposure combination, with 3 measurements per part in different locations and 20 scans taken per measurement. Tensile testing was carried out using a Hounsfield H25KS (Tinius Olsen Ltd, UK) Universal Testing Machine. Due to the constraints on printed sample dimensions previously mentioned, tensile testing was conducted following a modified version of the ISO 527 [31] standard with an extensometer used to measure strain. Dog bone samples were loaded into the grips with a separation of 45 mm. The test was run with an extensional rate of 1 mm/s. Five repeats ($n = 5$) for each measurement were taken. Hardness testing was performed following the BS EN ISO-6507 [32] and ISO/TS 19278:2019 [33] standards. An Innova Test Vickers hardness testing rig (Innova Test, the Netherlands) was used to indent and measure the hardness. Four repeats were carried out on three printed samples ($n = 12$) for each exposure level and material. A load of 200-g force and a dwell time of 15 s were used. For repeatability, a pyramidal indenter was pressed into the build plate surface of the horizontal build samples,

Table 5 Radiation doses for 3D printed parts

Radiation level (MGy)	PETG		ASA	
	Dose (MGy)	Rate (Gy/min)	Dose (MGy)	Rate (Gy/min)
0	None	–	None	–
1	0.75	35	0.75	35.5
2	1.5	69	1.5	71.5
3	2.25	110	2.25	103.5

and the diagonal length was measured using a microscope to calculate hardness. Following mechanical testing, the fracture surface was inspected visually.

Results

Infrared spectroscopy

Infrared transmission spectra of PETG and ASA before and after the various amounts of gamma exposure are shown in Fig. 4, with key peaks itemised in Table 6. Data sets are offset from one another, and the y-axis marking denotes 10% increments of transmission. For PETG samples following irradiation, a new broad peak at 3293 cm^{-1} corresponding to a hydroxyl group OH bond [25, 34] was observed. Peaks associated with C–H stretching, 2855–2925 cm^{-1}, and C–H bending, 1408 cm^{-1}, showed an increase in absorption (reduced transmission) at the highest exposure level suggesting the formation of C–H bonds. For most of the other listed bonds, there was no clear trend of increased or decreased absorption with exposure over 0.75 MGy.

For ASA, the only new peak formation was observed at the 3300 cm^{-1} wavelength associated with an OH bond [25]. The 2293 cm^{-1} peak associated with the C≡N bond maintained the peak intensity with exposure. This is expected as triple bonds are considerably stronger than saturated bonds [35]. All other peaks decreased in intensity at the 0.75 MGy exposure level and remained lower than the control sample intensity up to the 2.25 MGy exposure level.

Mechanical testing of PETG and ASA

Stress–strain curves from tensile testing for all PETG and ASA samples have been overlaid and are presented in Fig. 5. Results for horizontal build (primarily representative of material tensile strength) and vertical build (primarily representative of layer adhesion strength) are plotted on separate graphs. Increasing exposure has been offset on the strain axis to allow for the comparison of the data at different radiation exposure levels.

Regardless of the choice of material or degree of exposure to radiation, the levels of stress and strain
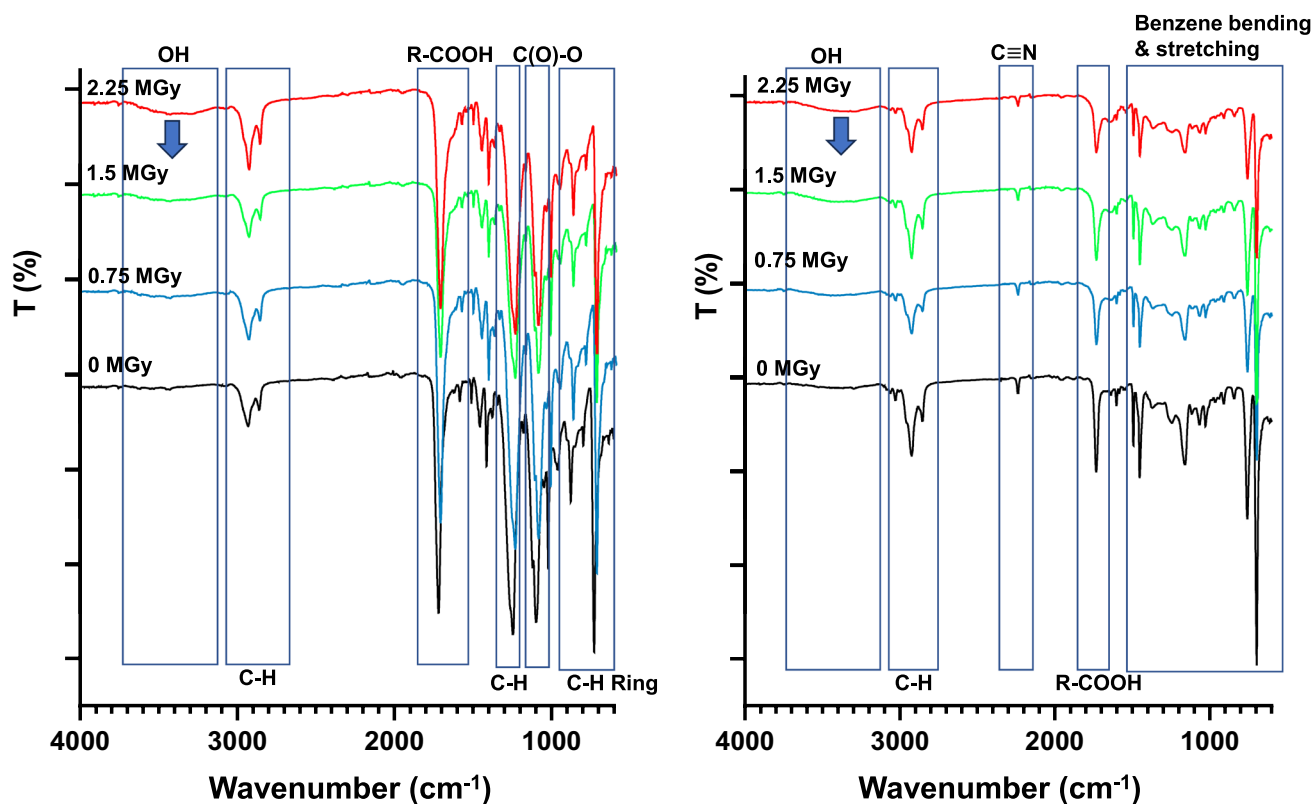

Figure 4 Infrared transmission spectra of PETG (left) and ASA (right). Wave numbers corresponding to specific bonds have been labelled, and arrows indicated broad absorption at ~ 3300 cm^{-1}.

Table 6 Key peaks from FT-IR analysis of PETG and ASA

Material	Bond	Wave number (cm^{-1})	Transmission (%) at radiation exposure (MGy)			
			0.0	0.75	1.5	2.25
PETG	Ring C–H	724	70.74	69.12	77.09	72.23
	C–H stretching cyclohexylene ring	956	89.83	88.4	91.58	89.39
	Ester C(O)–O stretching	1240	72.46	71.64	79.63	74.28
	C–H bending	1408	90.21	89.45	90.2	76.85
	Carbocyclic acid R–COOH	1712	74.79	74.39	81.76	71.12
	C–H stretching	2855	96.28	95.66	96.29	94.14
		2925	94.58	93.63	94.44	91.5
	OH Hydroxyl	3293	None	98	98.17	97.27
ASA	Benzene stretching	698	69.36	81.13	77.35	82.67
		758	84.98	90.66	88.79	91.1
	Benzene bending	1452	89.24	93.21	91.91	93.5
		1494	92.64	95.45	94.71	95.67
		1602	96.98	97.89	97.25	97.37
	Carbocyclic acid R–COOH	1733	89.98	93.52	92.5	93.92
	C≡N	2239	98.17	98.86	98.47	98.88
	C–H stretching	2853	95.34	97.1	95.82	96.32
		2923	91.67	94.73	92.67	93.94
	OH	3300	None	98.78	98.66	98.24

at failure were substantially lower for the vertical build than the horizontal build, with the former more indicative of the strength of the filament, and the primarily indicative of the strength of adhesion between filaments. ASA samples generally showed lower levels of stress and strain at failure than their PETG counterparts. Non-irradiated horizontal build samples demonstrated signs of ductile behaviour with plastic deformation prior to fracture, as reported elsewhere [36]. Following irradiation, the horizontal build samples transitioned to a more brittle failure mechanism. Non-irradiated and irradiated vertical build samples demonstrated brittle failure, lacking plastic deformation, regardless of whether they had been exposed to radiation, as reported in the previous literature [37].

The key mechanical properties (UTS, maximum strain, Young's modulus and hardness) and their response to gamma radiation are summarised in Fig. 6, there was some variability in the repetitions but compared to supplier data (Table 3) the UTS recorded for both materials was lower than quoted for horizontal builds, and the maximum strain for PETG was lower and for ASA higher than quoted. The Young's modulus was slightly higher than the quoted value for both materials. For vertical builds, the ASA UTS and maximum strain were lower while the Young's modulus

was in line with the quoted values. The largest discrepancy between supplier properties and those measured were for vertical build PETG where the measured maximum strain was only 16% of the quoted value, measured 32.8 MPa versus quoted 42 MPa. Generally, there is more variance in vertical build results when compared to horizontal.

Following exposure to radiation, prints using both materials and build orientations decreased in UTS and maximum strain with increasing exposure to gamma radiation. PETG horizontal build maintained a UTS of 32 MPa until 0.75 MGy, ultimately dropping to 9 MPa at 2.25 MGy. ASA horizontal builds reduced significantly in UTS from 30 MPa unexposed to 10 MPa at 0.75 MGy and ultimately reduced to 4 MPa at 2.25 MGy. As previously mentioned, vertical build samples achieved significantly lower UTS when compared to horizontal build yet suffered a similar pattern in terms of decreasing UTS with exposure to radiation, with PETG reducing from 5.3 to 2.7 MPa at 2.2 5 MGy and ASA reducing from 4.2 to 1.7 MPa at 1.5 MGy. For both materials, the maximum strain reduced with exposure to radiation. PETG horizontal builds reduced from 3.9% maximum strain to 0.46% at 2.25 MGy, while ASA reduced in maximum strain significantly from 5.3 to 0.5% at 0.75 MGy, ultimately reducing to
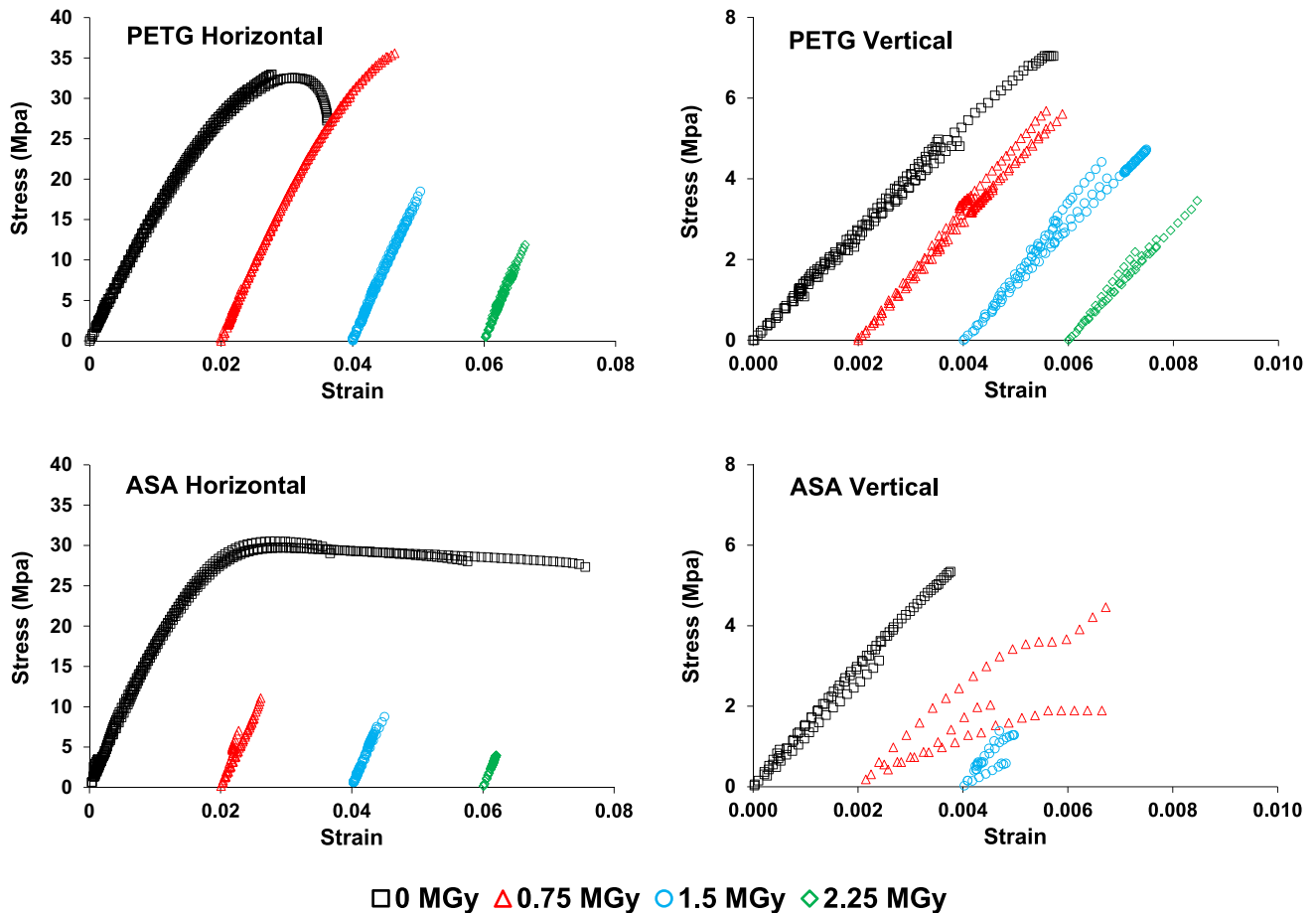
Figure 5 Stress–strain data for PETG and ASA materials printed at both horizontal and vertical orientations as a result of exposure to gamma radiation-increased exposure is offset on the strain axis.

0.17% at 2.25 MGy. Vertical build samples similarly reduced in maximum strain with PETG reducing from 0.41 to 0.18% at 2.25 MGy and for ASA from 0.29 to 0.10%. Young's modulus and hardness showed either modest increases or a fairly flat response with exposure. However, the variability in repeat measurements makes it difficult to conclude the true effect radiation has had on the elastic and hardness properties of the materials.

Observations of fracture surfaces

Images of fractured 3D printed samples are shown for PETG with horizontal and vertical builds in Figs. 7 and 8, respectively. Non-irradiated samples are compared to samples irradiated at the highest level (2.25 MGy). For PETG and ASA, the nature of the fracture for horizontal build samples changed

following irradiation. Non-irradiated samples, Fig. 7a & c, had rough surfaces, distinct infill and wall regions and evidence of thinning occurring after fracture, indicative of ductile failure. Following irradiation, Fig. 7b & d, fracture surfaces were flatter, smoother and showed no sign of local thinning, corresponding with observations from tensile testing and showing that gamma radiation-induced embrittlement in the material. For the vertical build, all fracture surfaces occurred between layer boundaries, creating flat fracture surfaces with no evidence of necking. From the front view images, the macrostructure of the deposition lines can be seen. There was no noticeable qualitative change in fracture behaviour as a result of radiation exposure; again, this corresponds with the consistent mode of brittle failure in the vertical build samples. Similar observations were made for ASA.
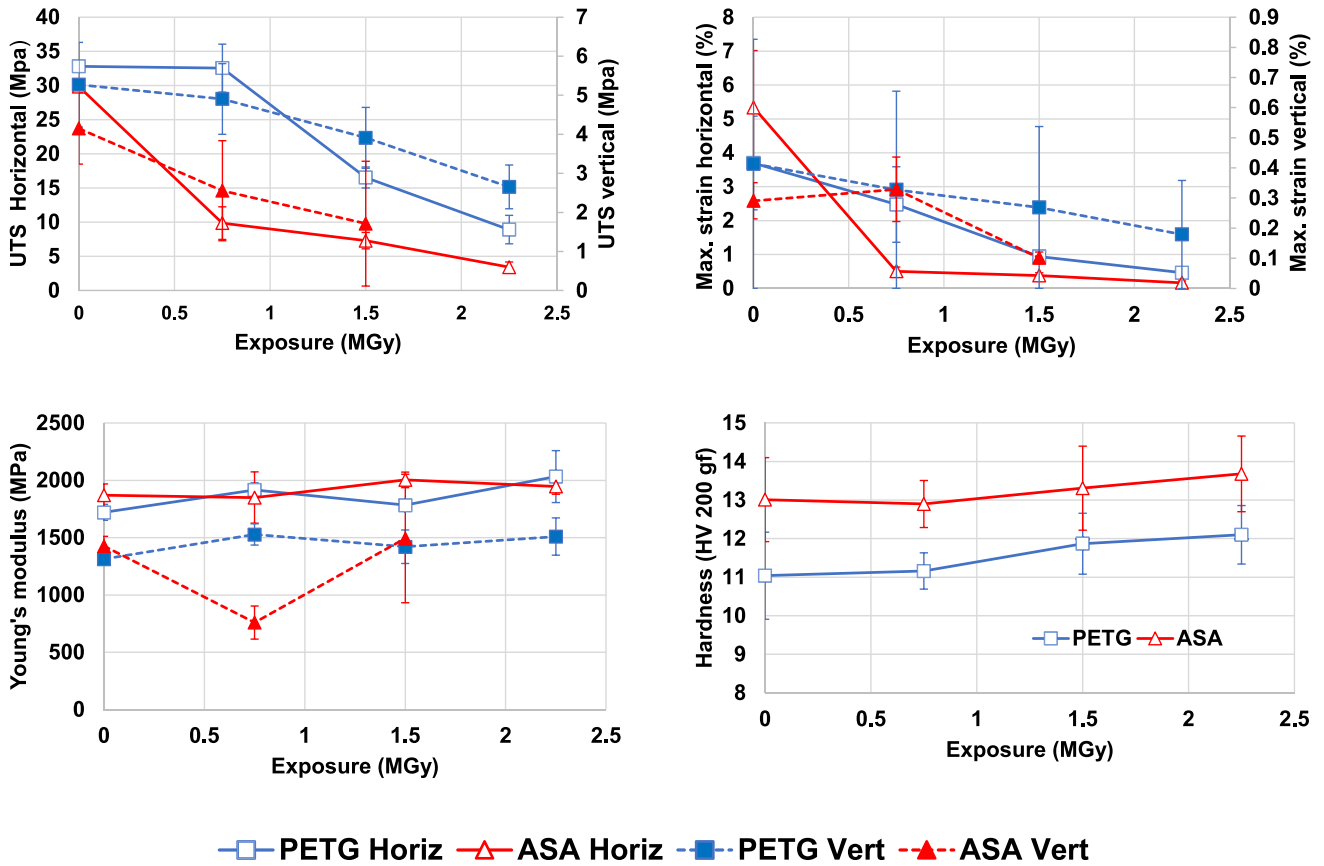
Figure 6 Change in mechanical properties with exposure to gamma radiation in terms of UTS (top left), maximum strain (top right), Young's modulus (bottom left) and hardness (bottom right).
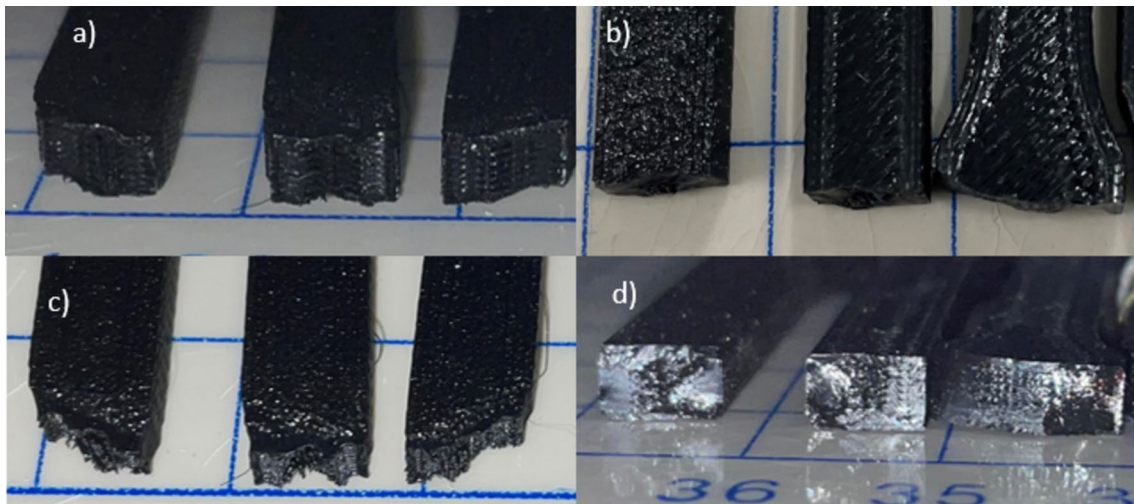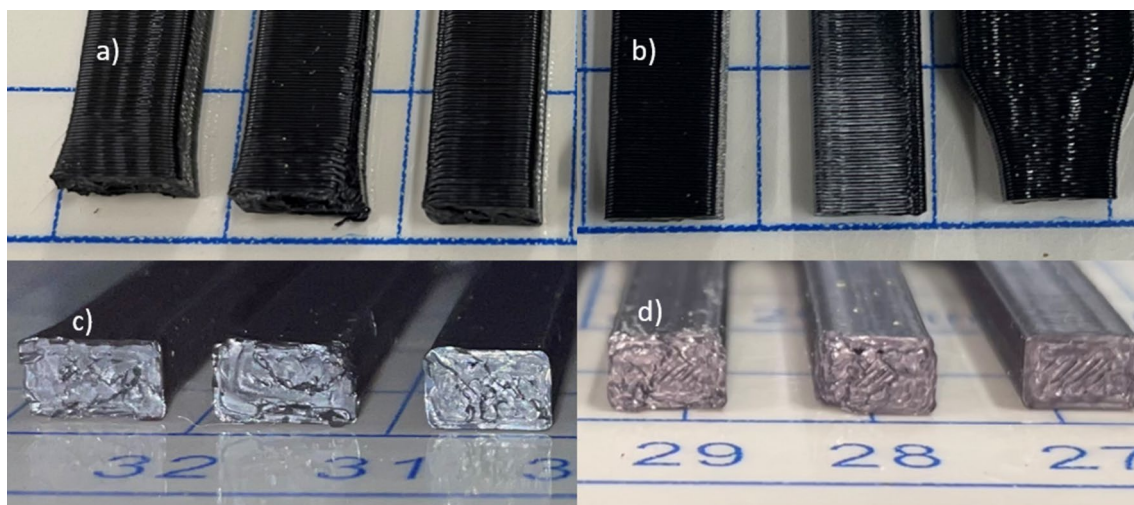

Figure 7 PETG horizontal build fracture surfaces—left (**a** & **c**) non-irradiated, right (**b** & **d**) irradiated with 2.25 MGy.

Figure 8 PETG vertical build fracture surfaces—left (**a** & **c**) non-irradiated, right (**b** & **d**) irradiated with 2.25 MGy.

Discussion

Infrared analysis suggested that exposure to gamma radiation altered the intermolecular bonding of the PETG and ASA polymers. The spectra suggest evidence of cross-linking occurring in both materials as indicated by the formation of the broad peak located at 3300 cm^{-1} corresponding to the hydroxyl group OH bond. From the PETG spectra, increases in peak intensity in bond corresponding to CH groups further indicate cross-linking through the radicalisation of hydrogen electrons, reforming new bonds and creating three-dimensional networks of polymer chains. For ASA, the decrease in other peak intensities could be an indication of chain scission breaking bonds along the polymer chain.

Research by others suggests that the AM fabrication process does not alter functional groups present in 3D printed parts when compared to bulk material [38]. However, gamma radiation has been shown to alter the intermolecular bonding within polymers [23], leading to cross-linking and chain scission. Cross-linking is known to induce embrittlement in the material, reducing the maximum strain at fracture yet increasing the Young's modulus [12]. In contrast, chain scission leads to a suppression of elastic properties, thus reducing Young's modulus [12]. Mechanical testing supports this cross-linking hypothesis, with embrittlement of the materials evidenced by a decrease in maximum strain but increase in Young's modulus. Additionally, chain scission is

expected to occur alongside cross-linking, evidenced by the decrease in tensile strength with increasing radiation exposure. Furthermore, visual inspection of the fracture surfaces following irradiation indicated the horizontal build failure modes transitioned towards brittle rather than ductile failure. Dose rates are quoted for air, and there will be attenuation of gamma radiation within any printed components depending on material, filament structure and thickness which will ultimately affect the mechanical behaviour. A study by Almeida et al. [43] shows attenuation of approximately 10% of incident gamma for 1 cm thick PLA and ABS printed with 100% infill.

Similar trends of reduction in tensile strength and strain at failure with radiation exposure were observed in the vertical build samples. However, these surfaces did not fundamentally change in the type of failure, being brittle in nature regardless. At the time of writing, there is no research into the effect of high levels of gamma radiation on the layer adhesion strength.

There are differences in mechanical properties measured between the work presented in this study and quoted results from supplier data sheets. All samples were fabricated using printing temperatures recommended by the supplier. However, other printing parameters, such as infill type, layer height, number of walls and print speed, were not indicated and were derived by experimental optimisation. It has been shown that changes in the printing parameters can drastically affect mechanical properties [39], and

compared with previous reported work for PETG and ASA, the horizontal (non-irradiated) PETG samples gave similar or lower UTS and only slightly lower maximum strain and Young's modulus [38, 40]. Previously published work for non-irradiated ASA samples gave similar or slightly higher UTS and higher maximum strain [41, 42] compared this study. Moreover, previous work has identified the difficulties in testing vertical build samples due to their fragile nature and inconsistency in layer adhesion at high Z coordinates [37]. Little research has been conducted on PETG or ASA samples printed in the vertical orientation. At the time of writing, no standard methodology is applied to tensile testing of 3D printed samples in terms of how the samples are produced and parameters such as raster angle and print temperature. While process parameters will affect the magnitude of the measured mechanical properties, the nature of the radiation-imposed changes should not be affected, and this test is a fair comparison of property changes that result from radiation exposure. A notable aspect of the mechanical data was a relatively high variability between many of the repeat measurements. This variability existed between unexposed as well as exposed samples. In some cases, the error bars overlapped, suggesting that there may not be a statistically significant difference between the materials or from the exposure.

Although there are no reported data on the robustness of PETG and ASA to radiation, previous studies exist on the effect of gamma radiation on PLA and ABS which can act as a benchmark. Comparing previous work investigating the radiation response of PLA and ABS to results from PETG and ASA in this study. Research has shown PLA to become unsuitable for functional use at exposure over 0.05 MGy [14, 15, 23]. In comparison, ABS has been shown to be more resistant to radiation, increasing in UTS and maximum strain at exposures lower than 0.05 kGy [26, 27]. However, at higher dosages, above 1 MGy, ABS significantly reduced in UTS and maximum strain. The data presented in this study demonstrate that PETG performs better than both PLA and ABS in mechanical testing after exposure to radiation, and ASA performs better than PLA and similarly to ABS. Note that direct comparison to previous work is difficult due to differences in dose rate and print parameter settings, i.e. work from [26] used thicker 2 mm walls. Ultimately, the results demonstrate the higher robustness of PETG to radiation, especially below 2 MGy, when compared to other similarly priced materials on the market.

Conclusions

The work presented in this paper investigates how the mechanical characteristics of 3D printed polyethylene terephthalate glycol (PETG) and acrylic styrene acrylonitrile (ASA) polymers respond to high doses of gamma radiation. The findings indicate that PETG outperforms ASA as well as PLA and ABS (reported historically). PETG maintains UTS up to 0.75 MGy and appears to be a suitable material from a robustness and cost-effective perspective for deployment in radioactive areas.

Infrared spectroscopy showed the evidence of polymer cross-linking as a result exposure to gamma radiation with the formation of peaks corresponding to –OH and C–H bonds. This is associated with a reduction in ultimate tensile stress and maximum strain in parts made from both polymers, but with PETG retaining greater strength and ductility than ASA, especially at intermediate gamma exposure. Young's modulus and hardness showed either modest increases or a fairly flat response with exposure. Mechanical properties were heavily dependent on the build structure, with the inherent strength of the material along the filament being several times greater than the fused layer adhesion strength. Non-irradiated samples pulled parallel to the filament direction showed ductile failure which transitioned to brittle failure with exposure to radiation. For samples pulled perpendicular to the filament direction, fractures occurred between layers, indicating brittle failure regardless of whether the samples were irradiated.

with the assistance of Ruth Edge from the University of Manchester at the Dalton Cumbrian Facility.

Author contributions

SC was involved in conceptualization, methodology, investigation and writing—original draft preparation, COP was responsible for supervision, visualisation, validation and writing—reviewing and editing, WAS contributed to writing— reviewing and editing, and methodology, and DD took part in conceptualisation, methodology, supervision, resources, validation, writing— reviewing and editing, and project administration.

Data and code availability

Not applicable.

Declarations

Conflict of interest   The authors declare that no conflicts of interest or competing interests exist.

Ethical approval   Not applicable.

References

[1] Guo N, Leu MC (2013) Additive manufacturing: technology, applications and research needs. Front Mech Eng 8(3):215–243. https://doi.org/10.1007/s11465-013-0248-8

[2] Petrovic V et al (2011) Additive layered manufacturing: sectors of industrial application shown through case studies. Int J Prod Res 49(4):1061–1079. https://doi.org/10.1080/00207540903479786

[3] da Silva Aquino KA (2012) Sterilization by gamma irradiation. Gamma Radiat 9:172–202. https://doi.org/10.5772/34901

[4] Bhat S (2020) 12–3D printing equipment in medicine. Elsevier, Singapore

[5] Martin H, Watson S, Lennox B, Poteau X (2018) Miniature inspection robot for restricted access exploration (MIRRAX), WM2018 Conference, pp 1–9

[6] Jones AR et al. (2017) On the design of a remotely-deployed detection system for reactor assessment at fukushima daiichi. In: 2016 IEEE nuclear science symposium, Medical imaging conference and room-temperature semiconductor detector workshop, NSS/MIC/RTSD 2016, pp 7–10. https://doi.org/10.1109/NSSMIC.2016.8069713

[7] Wong JY, Pfahnl AC (2014) 3D printing of surgical instruments for long-duration space missions. Aviat Space Environ Med 85(7):758–763. https://doi.org/10.3357/ASEM.3898.2014

[8] Rochus P, Plesseria JY, Van Elsen M, Kruth JP, Carrus R, Dormal T (2007) New applications of rapid prototyping and rapid manufacturing (RP/RM) technologies for space instrumentation. Acta Astronaut 61(1–6):352–359. https://doi.org/10.1016/j.actaastro.2007.01.004

[9] O'Donnell JH (1991) Chemistry of radiation degradation of polymers. In: Radiation effects on polymers, American Chemical Society, pp 402–413. https://doi.org/10.1021/bk-1991-0475.ch024

[10] Al-Sheikhly M, Christou A (1994) How radiation affects polymeric materials. IEEE Trans Reliab 43(4):551–556. https://doi.org/10.1109/24.370227

[11] Bhattacharya A (2000) Radiation and industrial polymers. Progress Polym Sci (Oxford) 25(3):371–401. https://doi.org/10.1016/S0079-6700(00)00009-5

[12] Makuuchi K, Cheng S (2011) Fundamentals of radiation crosslinking. In: Radiation processing of polymer materials and its industrial applications. John Wiley & Sons, Inc., pp 26–70. https://doi.org/10.1002/9781118162798.ch2

[13] Skiens W (1980) Mechanical properties of polymeric packaging films after radiation sterilization. Radiat Phys Chem 15:47–57

[14] Shaffer S, Yang K, Vargas J, Di Prima MA, Voit W (2014) On reducing anisotropy in 3D printed polymers via ionizing radiation. Polymer (Guildf) 55(23):5969–5979. https://doi.org/10.1016/j.polymer.2014.07.054

[15] West C, McTaggart R, Letcher T, Raynie D, Roy R (2019) Effects of gamma irradiation upon the mechanical and chemical properties of 3D-printed samples of polylactic acid. J Manuf Sci Eng Trans ASME 141(4):041002. https://doi.org/10.1115/1.4042581

[16] The ExoMars spacecraft measured radiation in deep space to help keep future astronauts safe. https://www.popsci.com/exomars-radiation-astronauts/. Accessed 25 May 2022

[17] Benton ER, Benton EV (2001) Space radiation dosimetry in low-Earth orbit and beyond. Nucl Instrum Methods Phys Res B 184(1–2):255–294. https://doi.org/10.1016/S0168-583X(01)00748-0

[18] Berger T (2008) Radiation dosimetry onboard the international space station ISS. Z Med Phys 18(4):265–275. https://doi.org/10.1016/j.zemedi.2008.06.014

[19] International Organization for Standardization BS EN ISO 11137-2-2013

[20] TEPCO (2022) Recent Topics: Tepco holdings sent robot into Fukushima Daiichi unit 2 reactor to clear path for later investigation with 'Scorpion' robot. https://www.tepco.co.jp/en/press/corp-com/release/2017/1375551_10469.html. Accessed 25 May 2022

[21] Backgrounder on radioactive waste|NRC.gov. https://www.nrc.gov/reading-rm/doc-collections/fact-sheets/radwaste.html#stor. Accessed 25 May 2022

[22] Lloyd WR, Sheaffer MK, Sutcliffe WG (1994) Dose rate estimates from irradiated light-water reactor fuel assemblies in air. U.S. Department of Energy Office of Scientific and Technical Information. https://www.osti.gov/servlets/purl/10137382

[23] Wady P et al (2020) Effect of ionising radiation on the mechanical and structural properties of 3D printed plastics. Addit Manuf 31:100907. https://doi.org/10.1016/j.addma.2019.100907

[24] Kim E, Shin YJ, Ahn SH (2016) The effects of moisture and temperature on the mechanical properties of additive manufacturing components: fused deposition modeling. Rapid Prototyp J 22(6):887–894. https://doi.org/10.1108/RPJ-08-2015-0095

[25] Benyathiar P (2014) Effect of ionizing irradiation techniques on biodegradable packaging materials. PhD thesis Michigan State University, p 253. https://doi.org/10.25335/M5ST6R

[26] Rankouhi B, Delfanian F, McTaggart R, Letcher T (2016) An experimental investigation of the effects of gamma radiation on 3D printed ABS for in-space manufacturing purposes. https://doi.org/10.1115/imece2016-67745

[27] Rankouhi B, Javadpour S, Delfanian F, McTaggart R, Letcher T (2018) Experimental investigation of mechanical performance and printability of gamma-irradiated additively manufactured ABS. J Mater Eng Perform 27(7):3643–3654. https://doi.org/10.1007/s11665-018-3463-y

[28] Kabanov VY, Feldman VI, Ershov BG, Polikarpov AI, Kiryukhin DP, Apel' PY (2009) Radiation chemistry of polymers. High Energy Chem 43(1):1–18. https://doi.org/10.1134/S0018143909010019

[29] Geon Kim D et al (2020) Performance of 3D printed plastic scintillators for gamma-ray detection. Nucl Eng Technol 52(12):2910–2917. https://doi.org/10.1016/j.net.2020.05.030

[30] Statista (2023) Worldwide most used 3D printing materials, as of July 2018. https://www.statista.com/statistics/800454/worldwide-most-used-3d-printing-materials/. Accessed 7 Jun 2023

[31] International Organization for Standardization (2018) BS EN ISO 527-3:2018

[32] International Organization for Standardization (2018) BS EN ISO 6507–1:2018

[33] International Organization for Standardization (2019) ISO-TS 19278-2019

[34] Dispenza C, Alessi S, Spadaro J (2017) Radiation processing of polymers in aqueous media. Appl Ioniz Radiat Mater Process 2:291–326

[35] Al-Sheikhly M, Christou A (1994) Tutorial how radiation affects polymeric materials. IEEE Trans Reliab 43(4):551–556. https://doi.org/10.1109/24.370227

[36] Guessasma S, Belhabib S, Nouri H (2019) Microstructure, thermal and mechanical behavior of 3D printed acrylonitrile styrene acrylate. Macromol Mater Eng 304(7):1–11. https://doi.org/10.1002/mame.201800793

[37] Szykiedans K, Credo W, Osiński D (2017) Selected mechanical properties of PETG 3-D prints. Procedia Eng 177:455–461. https://doi.org/10.1016/j.proeng.2017.02.245

[38] Santana L, Alves JL, Sabino Netto ADC, Merlini C (2018) A comparative study between PETG and PLA for 3D printing through thermal, chemical and mechanical characterization. Revista Materia 23(4):e22167. https://doi.org/10.1590/s1517-707620180004.0601

[39] Algarni M, Ghazali S (2021) Comparative study of the sensitivity of pla, abs, peek, and petg's mechanical properties to fdm printing process parameters. Crystals (Basel) 11(8):995. https://doi.org/10.3390/cryst11080995

[40] Modeling D et al (2021) Effect of printing parameters on the thermal and mechanical properties of 3D-printed PLA and PETG, using fused. Polymers 13:1–11

[41] Polymer additive manufacturing of ASA structure Influence of printing.pdf

[42] Grabowik C, Kalinowski K, Ćwikła G, Paprocka I, Kogut P (2017) Tensile tests of specimens made of selected group of the filament materials manufactured with FDM method. MATEC

Web Conf 112:04017. https://doi.org/10.1051/matecconf/201711204017

[43] Almeida JS, Villani D, Potiens MPA, Willegaigon J (2021) Dosimetric characterization of 3D printed for ^{137}Cs gamma rays. J Phys: Conf Ser 1826:012042. https://doi.org/10.1088/1742-6596/1826/1/012042